

PHYSICS

Recognitions of colored fabrics/laser-patterned metals based on photothermoelectric effects

Zekun Liu^{1,2†}, Zhenhua Wu^{1,2†}, Shuai Zhang^{1,2}, Yanxi Lv², Erzhen Mu³, Ruijie Liu⁴, Dongshi Zhang⁴, Zhuguo Li^{4,5}, Shibo Li⁶, Ke Xu⁷, Zhiyu Hu^{1*}

Color is the mapping of electromagnetic waves of different wavelengths in human vision. The electronic color recognition system currently in use is mainly based on the photoelectric effect. Here, we demonstrate a color materials' recognition system based on photothermoelectric effects. The system uses a microfabricated thermoelectric generator (TEG) as a platform, which is covered with dye-colored fabric pieces or structure-colored laser-patterned metal sheets. Under light irradiation, the fabrics/metals selectively absorb light and convert it into heat, which flows through the underlying TEG arrays and then converted into electrical signal output to realize the distinction of color and materials. This previously unidentified high-sensitivity TEG detection method provides a potential approach for precise color materials' detection over wide areas and may help understand the mechanism of bionic color recognition.

INTRODUCTION

Color is the visual expression of the interaction among light sources, matters, and observers (human eyes or sensors). It has three attributes, namely, hue, lightness, and purity. Different combinations of color attributes can form more than 7.5 million colors, and the number of colors recognizable to the human eye is estimated to be up to 2.7 million (1). Color recognition plays a very important role in wide fields, such as disease detections (2, 3), chemical reaction processes (4, 5), environmental protection (6, 7), sensing applications (8), industrial production (9), etc. In the past few decades, a great number of electronic apparatuses have been developed for color and optical recognition based on photoelectric effects, such as (photo-emissive) photomultiplier tube, cooled charge-coupled devices, or the (junction-based) avalanche photodiode for high-sensitivity detection (10).

Photons can be converted into electricity through the photoelectric effects and heat through the photothermal effects. Photothermal effects may offer additional information to understand the complex mechanisms of colors and materials. A thermoelectric generator (TEG) based on the Seebeck effect can convert the thermal signal to the electric output, providing another possibility for optical power measurement and color recognition (11, 12). The thermal voltage (ΔU) varies with the temperature changes (ΔT) as given by equation $nS = \Delta U/\Delta T$, where S is the sum Seebeck coefficient of a P-N thermoelectric pair and n is the number of thermoelectric pairs (13). TEG can be used as self-powered sensors by converting heat into direct current signals (14–16), such as biochemistry sensors (17)

(detection of a biomolecule immunoassay of α -fetoprotein), optical sensors (18–20) (solar intensity and multiband light from visible light to terahertz detection based on photothermoelectric effect combined with light absorber), etc. In general, the physical size and thermal mass of TEG determine its minimum sensitivity to small temperature changes (21). Recently, we reported a microfabricated microelectromechanical TEG (MEMS TEG) integrating more than 10,000 submicrometer-thick thermoelectric pairs and thus may demonstrate excellent thermal sensitivity (22, 23).

In this work, we have used this homemade MEMS TEG (integrates with 46,000 thermoelectric pairs) to detect photothermal effects caused by three dye-colored fabrics (linen/cotton/blending) and eight structure-colored laser-patterned metal sheets [fabricated by femtosecond laser ablation in air (FLAA)]. The fabrics and metals absorb light and convert it into heat that drives the underlying MEMS TEG and produces electrical signals to be recognized by the system (Fig. 1). This work provides a previously unidentified high-sensitivity MEMS TEG detection method for color recognition by thermal signal, which provides a different perspective for bionic color materials' recognition and potentially helps to understand the mechanism of bionic color recognition in the future.

RESULTS

MEMS TEG and colored fabrics

Figure 2 shows the MEMS TEG. The ultrathin structure and series integration mode provide very high-temperature sensitivity and extremely short response times attributed to the response time associated with heat transport through the micrometer-thick thin film. The thermal response time is about $4l^2/\pi^2D$, where l is the thickness of the thermoelement and D is the thermal diffusivity (24).

Color calibration of dye-colored fabrics was conducted to minimize the interference of the experiment. The 1976-L*a*b* chromaticity system recommended by the International Commission on Illumination was adopted for chromaticity analysis. The chromaticity difference (ΔE) is expressed in (25, 26)

$$\Delta E = \sqrt{(\Delta L^*)^2 + (\Delta a^*)^2 + (\Delta b^*)^2}$$

¹National Key Laboratory of Science and Technology on Micro/Nano Fabrication, Shanghai Jiao Tong University, Shanghai 200240, China. ²Department of Micro/Nano Electronics, School of Electronic Information and Electrical Engineering, Shanghai Jiao Tong University, Shanghai 200240, China. ³School of Materials Science and Engineering, Henan Polytechnic University, Henan 454003, China. ⁴Shanghai Key Laboratory of Materials Laser Processing and Modification, School of Materials Science and Engineering, Shanghai Jiao Tong University, Shanghai 200240, China. ⁵State Key Laboratory of Metal Matrix Composites, School of Materials Science and Engineering, Shanghai Jiao Tong University, Shanghai 200240, China. ⁶Department of Microelectronics Science and Engineering, School of Electronic Information and Electrical Engineering, Shanghai Jiao Tong University, Shanghai 200240, China. ⁷Zhiyuan College, Shanghai Jiao Tong University, Shanghai 200240, China.

*Corresponding author. Email: zhiyuhu@sjtu.edu.cn

†These authors contributed equally to this work.

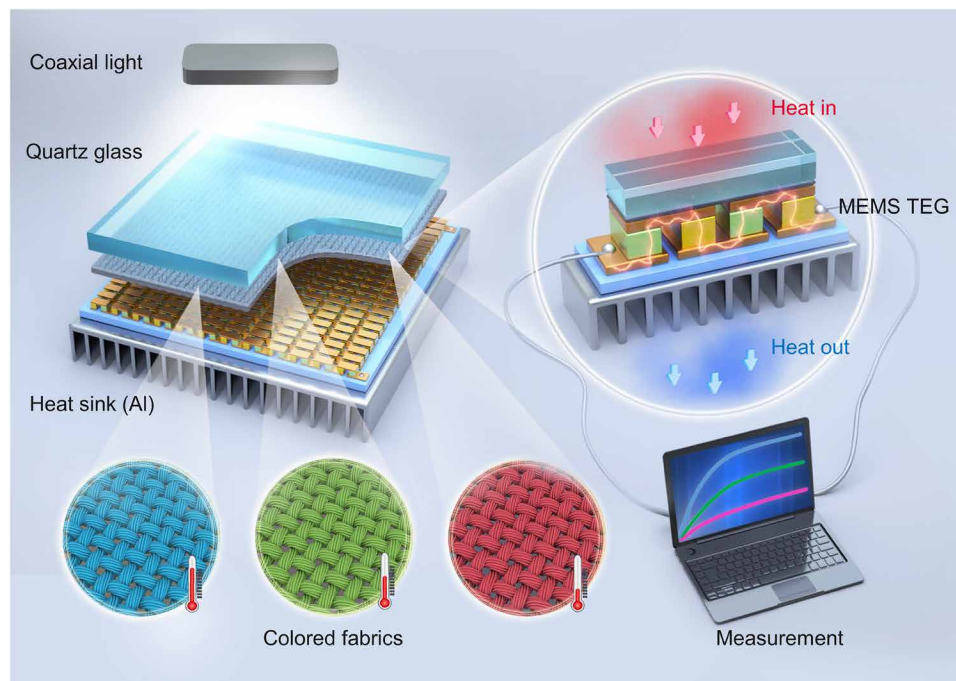


Fig. 1. Schematic illustration of the photothermoelectric-coupled color recognition platform based on MEMS TEG.

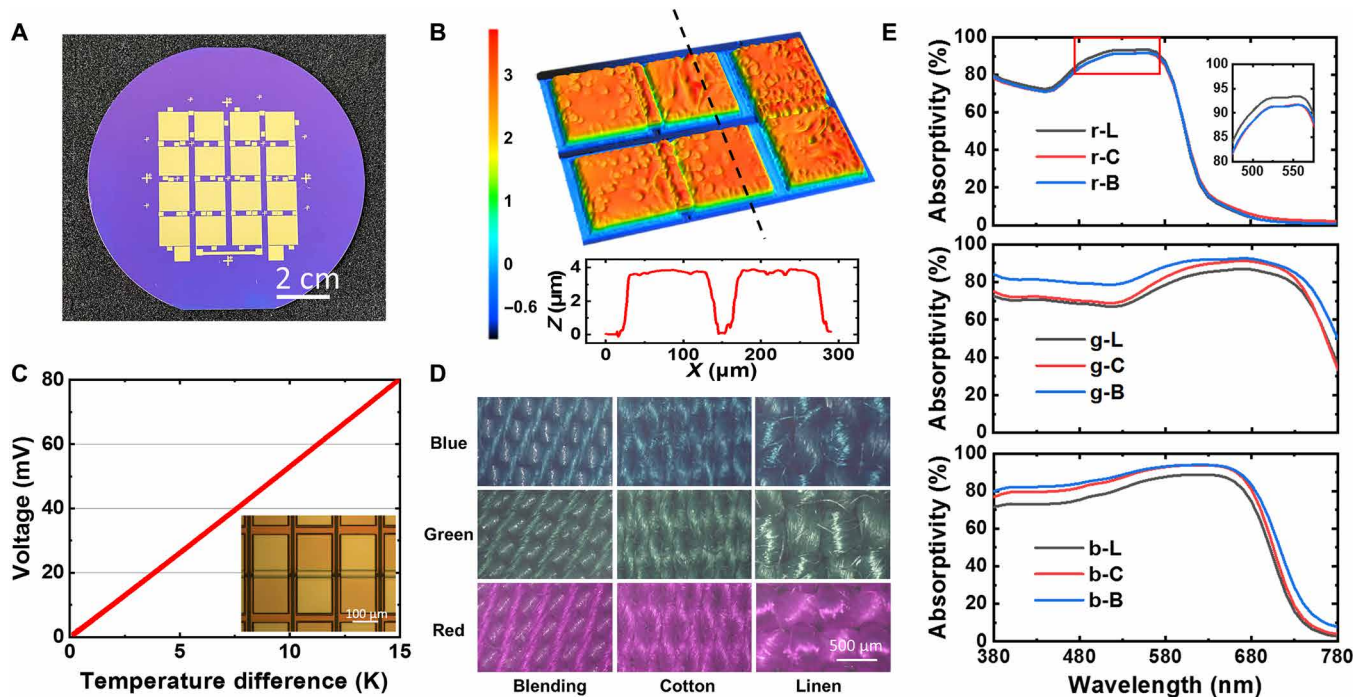


Fig. 2. Characterizations of MEMS TEG and fabrics. (A) Digital photo of MEMS TEG. (B) Morphology of P-N thermoelectric pairs. (C) Power performance. (D) Optical microscope photos of fabrics. (E) Absorptivity spectra in visible band (380 to 780 nm).

where L^* represents brightness and a^* and b^* are the chromaticity. The small ΔE value between the two fabrics indicates a similar hue. By ΔE comparison, nine samples in three groups were finally selected, which can support the next detection of photothermal effects of different fabrics with the same color. The corresponding ΔE

obtained was given in table S1. The L^* , a^* , and b^* values of each dye-colored fabric were given in table S2. The absorption spectra of the fabrics in the visible band (380 to 780 nm) are given in Fig. 2E. Fabrics of the same color have a similar trend in absorptivity, while the slight difference in value is due to the variance of

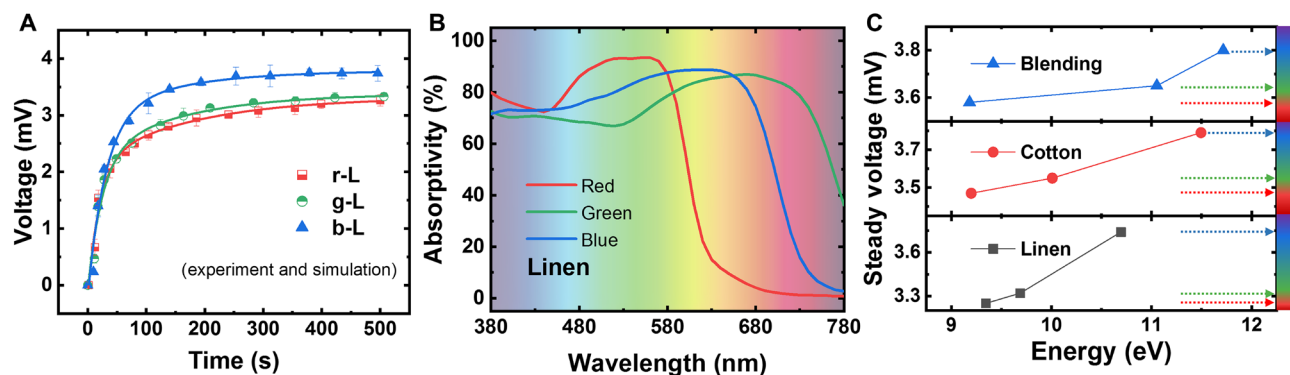


Fig. 3. Characterization of linen. (A) V_{oc} of MEMS TEG. (B) Absorptivity in the visible light band. (C) Comparison of incident light energy with V_{soc} .

materials. The samples are named by color material to simplify the description of the fabrics.

Color fabric identification

Taking the linen fabric as an example, as the illumination time increases, the colored fabric absorbs light energy and partly converts it into heat energy, the temperature gradually increases, and the open-circuit voltage (V_{oc}) of the MEMS TEG output gradually increases (Fig. 3A). Then, as the temperature rises, heat radiation and other heat dissipation effects are improved, and the voltage gradually tends to be stable, indicating that the system reaches thermal equilibrium at this time. The steady-state V_{oc} (V_{soc}) is an important parameter based on MEMS TEG for comparing the photothermoelectric capacity of colored matter and is also the main index for color discrimination. For the three colors of linen, V_{oc} increases rapidly at first and then gradually stabilizes, and the V_{soc} of three fabrics are $V_{b-L} = 3.74$ mV, $V_{g-L} = 3.32$ mV, and $V_{r-L} = 3.25$ mV, respectively, in descending order. This shows that the temperature difference generated from the photothermal conversion of different fabrics is $\Delta T_{blue} > \Delta T_{green} > \Delta T_{red}$, indicating the feasibility of identifying materials of different colors through the photothermoelectric effect. The response time t_{75} (time of V_{oc} from 0 to $0.75 V_{soc}$) is essentially in the limited range for the same material, while there is a sequence of linen, cotton, and blending from larger to smaller (fig. S1). The specific data are shown in the Supplementary Materials (table S3 and fig. S1).

It is well known that colored materials absorb one wave band of light in visible light and reflect the rest. This selective partial absorption of visible light makes it present a complementary color of visible light (27). The absorptivity of three different colored linen samples in a visible light band are shown in Fig. 3B. The energy corresponding to wavelength can be obtained as follows

$$E = \frac{hc}{\lambda}$$

where h is Planck's constant and c is the speed of light. The sum of the light energy absorbed by the colored fabrics under illumination is obtained through numerical integration of the relevant energy range. This integral value corresponds to the steady-state thermal voltage of the fabrics, indicating that for fabrics of the same materials but different colors, the sum energy positively correlates with its steady-state

voltage. This verifies the rationality of the thermal voltage sequence from the perspective of absorptivity. The three fabrics selected in this work are all in line with the above description (Fig. 3C). The wavelength-absorptivity and energy-absorptivity relations of cotton and blending fabrics are given in figs. S2 and S3.

Figure 4 (A and B) compares the V_{soc} generated by the MEMS TEG under the colored fabrics when illuminated. The V_{soc} order means that blue fabric has a better photothermal effect than green and red. This phenomenon exists in all three kinds of fabrics, which can be explained by the absorption of light energy by colored fabrics. Colored linen was selected to study the effect of light concentration on fabric detection. The results showed that V_{soc} increased linearly with light intensity for all three colored linen fabrics (fig. S4). The distinction of more colored cotton fabrics is given in fig. S5. V_{soc} of fabrics with the same color is blending, cotton, and linen in descending order. This result means that MEMS TEG-based system can recognize materials in addition to distinguishing colors.

Pattern metals' distinction and potential extension

To expand the applicability of this technology, we selected laser-patterned metals that have either a colorful iridescence or a black color, which are excellent biomimetic interfaces (28–31), as the object to identify. There are also dissimilarities in the V_{soc} of laser-patterned metals with different materials and structures, which means that it can also discriminate materials with structural colors. The scanning electron microscopy (SEM) images and corresponding V_{soc} under the same lighting condition are shown in Fig. 4 (D and E). Three-dimensional (3D)-printed microstructured metal sheets (steel and aluminum) with different structures can also be distinguished (fig. S6).

To further explore the potential application of MEMS TEG for identification, variable powered all solid-state low-noise lasers were used to irradiate MEMS TEG covered with polydimethylsiloxane/ Al_2O_3/SiO_2 . This structurally designed material has a low overall absorptivity and a relatively noticeable change in visible band (fig. S7), which is useful for detecting small energy changes caused by power changes of the laser. The V_{soc} and the laser power show a strong linear correlation under the laser irradiation of three wavelengths (Fig. 4C). For lasers with different wavelengths, the V_{soc} gradient (k) is consistent with the laser energy (E), and the ratio $\left(\frac{k_{405}}{E_{405}} : \frac{k_{532}}{E_{532}} : \frac{k_{727}}{E_{727}}\right)$ is 1:0.989:1.022 (table S4). This proves that MEMS TEG can also achieve effective resolution for fixed wavelength laser irradiation.

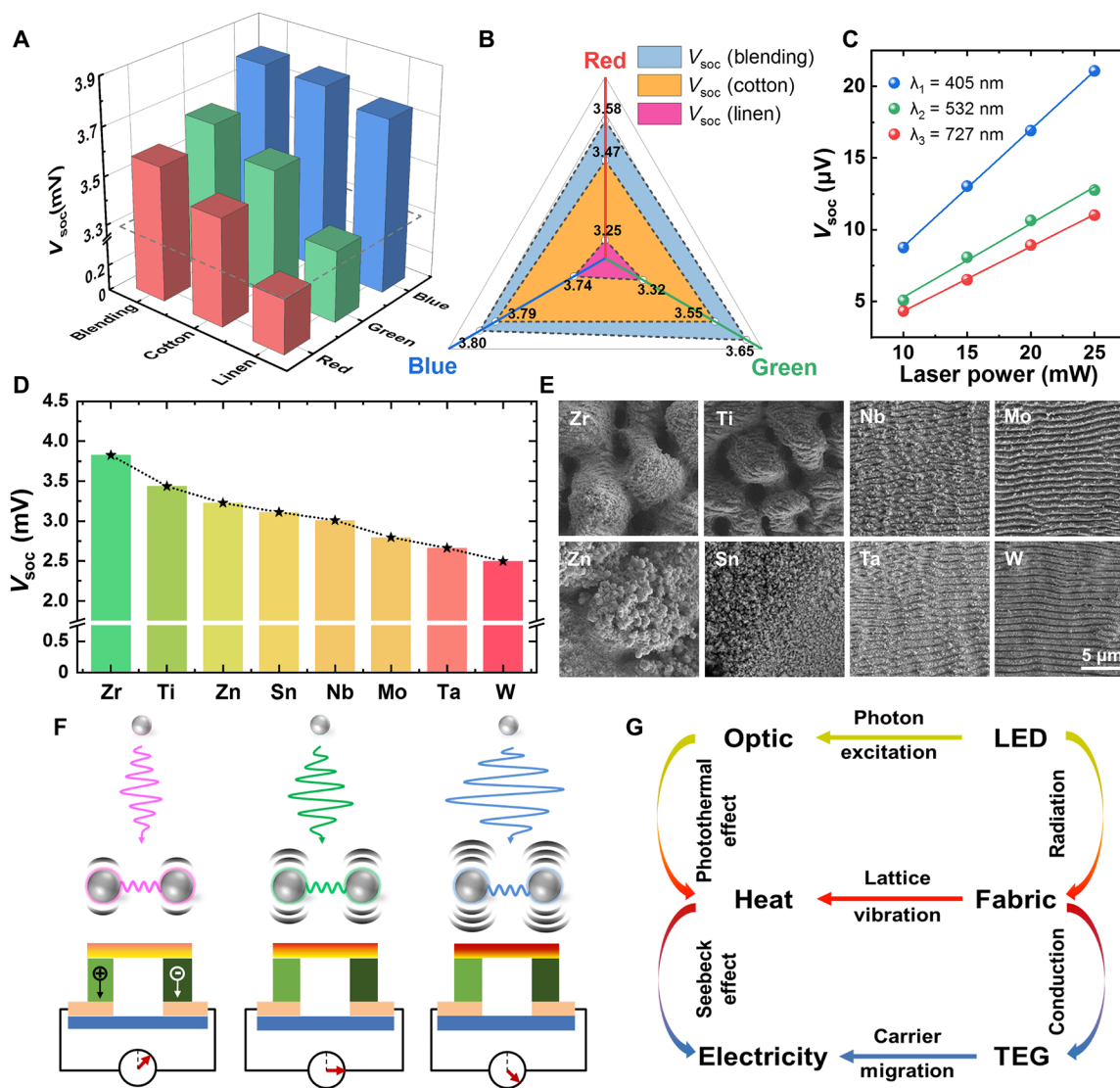


Fig. 4. V_{soc} comparison of MEMS TEG. (A and B) Colored fabrics. (C) PDMS/Ag/SiO₂ (under laser irradiation). (D) Laser-patterned metal sheets (Zr, Ti, Zn, Sn, Nb, Mo, Ta, and W) with (E) SEM images under the same magnification. (F and G) Schematic illustration of materials and energy in the system. LED, light-emitting diode.

DISCUSSION

Figure 4 (F and G) shows the energy conversion process of the system and explains the interaction relation of materials and light from the physical perspective. Under the same illumination condition, the vibration of atoms or molecules is enhanced because of the selective absorption of light by fabrics of different colors. Among them, the vibration of atoms in the blue fabrics is the strongest, and in that of the red fabrics is the weakest. Correspondingly, the blue fabrics generated the most heat, and the thermal voltage produced by MEMS TEG is the highest under the same heat dissipation condition. Similarly, the recognition process due to different light absorption and conversion capabilities. This proves the rationality and theoretical basis of MEMS TEG-based photothermoelectric color materials' recognition. Apart from that, its micrometer-scale thickness gives it outstanding advantages in terms of thermal sensitivity and response speed. This

enables future construction of excellent detection systems beyond those mentioned in this work, such as biochemical reactions, physical state changes, etc. (12, 32).

In summary, a photothermoelectric color materials' recognition system is designed here. MEMS TEG is used as a bridge, which allows the energy to change from light to heat and then to electricity, and then realizes the resolution of different colored fabrics or laser-patterned/3D-printed metals through electrical signals. For monochromatic fabrics, millivolt-level V_{oc} s depending on color and materials can be obtained with one-ninth of the standard solar intensity without boosting circuits. The accurate resolution of the electrical signal difference of 0.01 mV illustrates the sensitivity of the thermoelectric device with a temperature difference of 10^{-3} K, which indicates the potential for high-precision temperature measurement and sensors. This work proposes a simple and sensitive recognition system, which provides a previously unknown approach for color recognition by

thermal signal. It may have the potential for application in bionic color materials' sensors, process heat changes monitoring, and other fields.

MATERIALS AND METHODS

Fabrication of MEMS TEG

MEMS TEG with π -type P-N pair series perpendicular to the substrate was fabricated to detect the heat variation. The main fabricated process includes ultraviolet (UV) lithography, liftoff, and magnetron sputtering. Magnetron sputtering (TRP-450, SKY, China) was used to deposit thermoelectric materials and metal electrodes. UV lithography (SUSS MA6, Hoffmann Instruments, Germany) was used to realize the patterning of the bottom electrode, thermoelectric (TE) material, supporting glue, and top electrode in five steps.

A 4-inch SiO_2/Si was used as the substrate of TEG. Sb_2Te_3 and Bi_2Te_3 were selected as p-type and n-type thermoelectric materials, respectively. Cu was chosen as the electrode material for its excellent electrical and thermal conductivity. The noncontact lithography and photoresist melting technology were adopted to ensure that the interface between the electrode, the thermoelectric legs, and the supporting glue is smooth to obtain a good electric contact. The morphology and 3D topography of MEMS TEG were captured by optical microscopy (Axio Lab.A1, Zeiss, Germany) and laser scanning confocal microscope (VK-X3000, Keyence, USA). The specific processing details have been reported in our previous studies (22, 33).

Preparation of dye-colored fabrics and structure-colored metals

To obtain colored fabrics with similar chromaticity, a dyeing-selective process was designed. Reactive dyes were used to color pure white cotton, linen, and blended fabrics. In the process, dye molecules react with amino groups in protein fibers and hydroxyl groups in cellulose to form a whole with high colorfastness. The color fixing agent is sodium carbonate, and the dye aid is sodium chloride. According to the dyeing effect of different fabrics on the dye solution, the concentration of 6, 8, 10, 12, and 14 mg/ml of the dye solution is configured to facilitate subsequent screening according to the chroma data. The amounts of cosolvent/dyeing agent/fixing agent and dyeing/fixing temperature were unified. The specific dyeing steps are given in the Supplementary Materials. A UV-visible near-infrared spectrophotometer (Lambda 950, PerkinElmer, USA) was used to detect the chromaticity of fabrics dyed with different concentrations of dye solution. Last, the fabrics were standardized to a size of 5 cm by 5 cm for subsequent testing.

The laser-induced periodic surface structure (LIPSS) on various metals was manufactured using FLAA to form the structure-colored laser-patterned sheets. A femtosecond laser (pulse duration of 400 fs, wavelength of 1030 nm, power of 8 W, and repetition rate of 400 kHz) was used for the FLAA of Sn, Ta, Mo, Nb, W, Ti, Al, Zn, and Zr. The samples were scanned at a scan speed of 200 mm s^{-1} by a high-speed galvanometer scanner, and the scan line intervals were set at $15 \mu\text{m}$. The surface morphologies were characterized by SEM (NOVA NanoSEM 230, FEI, USA). The specific processing details have been reported in our previous studies (30).

Construction of detection system

To realize the recognition of color, the components of the detection system from top to bottom are a light source, quartz glass, fabrics or metals, MEMS TEG, heat sink, and data acquisition instrument

(Fig. 1). Specifically, the light source uses three-color light-emitting diode coaxial light (COS80-RGBWJF-M, CST, China), which can form monochromatic light in a narrow band and generate uniform parallel light through the designed light path. The fabrics or metals to be detected were directly placed on the surface of the MEMS TEG, and the light intensity received by samples is 115 W/m^2 tested by a solar power meter (TES-132, TES, China), which is about one-ninth of the standard light intensity (1000 W/m^2). To reduce the extra thermal contact resistance caused by the flexible characteristics of the fabric samples, the same quartz glass (Alfaquartz, China) was placed on the surface of the fabrics during the test. In addition, the platform was sealed to minimize the influence of convection heat transfer caused by airflow, so the heat dissipation conditions could be considered the same. Each sample was detected three times and averaged. After each test, the system was cooled to room temperature naturally.

SUPPLEMENTARY MATERIALS

Supplementary material for this article is available at <https://science.org/doi/10.1126/sciadv.abo7500>

REFERENCES AND NOTES

1. K. Nassau, The fifteen causes of color: The physics and chemistry of color. *Color Res. Appl.* **12**, 4–26 (1987).
2. S. E. Chou, K. L. Lee, P. K. Wei, J. Y. Cheng, Screening anti-metastasis drugs by cell adhesion-induced color change in a biochip. *Lab Chip* **21**, 2955–2970 (2021).
3. K. M. Cooper, R. T. Hanlon, B. U. Budelmann, Physiological color change in squid iridophores. *Cell Tissue Res.* **259**, 15–24 (1990).
4. J. Cui, J. E. Kwon, H. J. Kim, D. R. Whang, S. Y. Park, Smart fluorescent nanoparticles in water showing temperature-dependent ratiometric fluorescence color change. *ACS Appl. Mater. Interfaces* **9**, 2883–2890 (2017).
5. M. J. Shin, Relationship of color change to permeation of target compound in polydiacetylene vesicle system. *J. Appl. Polym. Sci.* **138**, 51192 (2021).
6. V. Kumar, Light scattering and consequent color change in Lukha River due to suspended aluminosilicate particles during winter months. *Int. J. Energy Water. Resour.* **6**, 121–132 (2021).
7. L. S. Mills, E. V. Bragina, A. V. Kumar, M. Zimova, D. J. R. Lafferty, J. Feltner, B. M. Davis, K. Hacklander, P. C. Alves, J. M. Good, J. Melo-Ferreira, A. Dietz, A. V. Abramov, N. Lopatina, K. Fay, Winter color polymorphisms identify global hot spots for evolutionary rescue from climate change. *Science* **359**, 1033–1036 (2018).
8. R. Zhang, Z. Yang, X. Zheng, Y. Zhang, Q. Wang, Large-strain and full-color change photonic crystal films used as mechanochromic strain sensors. *J. Mater. Sci. Mater. Electron.* **32**, 15586–15593 (2021).
9. N. Yüzer, F. Aköz, L. D. Öztürk, Compressive strength-color change relation in mortars at high temperature. *Cem. Concr. Res.* **34**, 1803–1807 (2004).
10. R. A. Yotter, D. M. Wilson, A review of photodetectors for sensing light-emitting reporters in biological systems. *IEEE Sens. J.* **3**, 288–303 (2003).
11. Z. Hu, Z. Wu, *Nanostructured Thermoelectric Films* (Shanghai Jiao Tong Univ. Press, 2020).
12. Z. Wu, S. Zhang, Z. Liu, E. Mu, Z. Hu, Thermoelectric converter: Strategies from materials to device application. *Nano Energy* **91**, 106692 (2022).
13. G. J. Snyder, E. S. Toberer, Complex thermoelectric materials. *Nat. Mater.* **7**, 105–114 (2008).
14. W. Li, Z. Ni, J. Wang, X. Li, A front-side microfabricated tiny-size thermopile infrared detector with high sensitivity and fast response. *IEEE Trans. Electron Devices* **66**, 2230–2237 (2019).
15. X. Cai, A. B. Sushkov, R. J. Suess, M. M. Jadidi, G. S. Jenkins, L. O. Nyakiti, R. L. Myers-Ward, S. Li, J. Yan, D. K. Gaskill, T. E. Murphy, H. D. Drew, M. S. Fuhrer, Sensitive room-temperature terahertz detection via the photothermoelectric effect in graphene. *Nat. Nanotechnol.* **9**, 814–819 (2014).
16. Z. Wang, P. Erhart, T. Li, Z. Zhang, D. Sampedro, Z. Hu, H. A. Wegner, O. Brummel, J. Libuda, M. B. Nielsen, K. Moth-Poulsen, Storing energy with molecular photoisomers. *Joule* **5**, 3116–3136 (2021).
17. L. Huang, J. Chen, Z. Yu, D. Tang, Self-powered temperature sensor with Seebeck effect transduction for photothermal-thermoelectric coupled immunoassay. *Anal. Chem.* **92**, 2809–2814 (2020).
18. A. Safaei, S. Chandra, M. W. Shabbir, M. N. Leuenberger, D. Chanda, Dirac plasmon-assisted asymmetric hot carrier generation for room-temperature infrared detection. *Nat. Commun.* **10**, 3498 (2019).

19. W. Zhu, Y. Deng, L. Cao, Light-concentrated solar generator and sensor based on flexible thin-film thermoelectric device. *Nano Energy* **34**, 463–471 (2017).
20. M. Zhang, D. Ban, C. Xu, J. T. W. Yeow, Large-area and broadband thermoelectric infrared detection in a carbon nanotube black-body absorber. *ACS Nano* **13**, 13285–13292 (2019).
21. Z. Wu, G. Yang, E. Mu, Q. Wang, S. A. Meijer, Z. Hu, Nanofire and scale effects of heat. *Nano Converg.* **6**, 5 (2019).
22. E. Mu, Z. Wu, Z. Wu, X. Chen, Y. Liu, X. Fu, Z. Hu, A novel self-powering ultrathin TEG device based on micro/nano emitter for radiative cooling. *Nano Energy* **55**, 494–500 (2019).
23. Y. Liu, E. Mu, Z. Wu, Z. Chen, F. Sun, X. Fu, F. Wang, X. Wang, Z. Hu, Ultrathin MEMS thermoelectric generator with Bi₂Te₃(Pt, Au) multilayers and Sb₂Te₃ legs. *Nano Converg.* **7**, 8 (2020).
24. R. Venkatasubramanian, E. Siivola, T. Colpitts, B. O'Quinn, Thin-film thermoelectric devices with high room-temperature figures of merit. *Nature* **413**, 597–602 (2001).
25. K. McLaren, XIII—The development of the CIE 1976 (L*a*b*) uniform colour space and colour-difference formula. *J. Soc. Dye. Colour* **92**, 338–341 (1976).
26. R. G. Kuehni, Color-tolerance data and the tentative CIE 1976 L*a*b* formula. *J. Opt. Soc. Am.* **66**, 497–500 (1976).
27. J. Griffiths, *Colour and Constitution of Organic Molecules* (Academic Press, 1976).
28. D. Zhang, B. Ranjan, T. Tanaka, K. Sugioka, Carbonized hybrid micro/nanostructured metasurfaces produced by femtosecond laser ablation in organic solvents for biomimetic antireflective surfaces. *ACS Appl. Nano Mater.* **3**, 1855–1871 (2020).
29. E. Skoulas, A. Manousaki, C. Fotakis, E. Stratakis, Biomimetic surface structuring using cylindrical vector femtosecond laser beams. *Sci. Rep.* **7**, 45114 (2017).
30. D. Zhang, R. Liu, Z. Li, Irregular LIPSS produced on metals by single linearly polarized femtosecond laser. *Int. J. Extreme Manuf.* **4**, 015102 (2022).
31. R. Liu, D. Zhang, Z. Li, Femtosecond laser induced simultaneous functional nanomaterial synthesis, in situ deposition and hierarchical LIPSS nanostructuring for tunable antireflectance and iridescence applications. *J. Mater. Sci. Technol.* **89**, 179–185 (2021).
32. Z. Wu, Z. Hu, Perspective—Powerful micro/nano-scale heat engine: Thermoelectric converter on chip. *ECS Sens. Plus* **1**, 023402 (2022).
33. E. Mu, G. Yang, X. Fu, F. Wang, Z. Hu, Fabrication and characterization of ultrathin thermoelectric device for energy conversion. *J. Power Sources* **394**, 17–25 (2018).

Acknowledgments: We would like to thank the Center of Advanced Electronic Materials and Devices (AEMD) and the Instrumental Analysis Center of Shanghai Jiao Tong University for providing experimental support. We also thank Y. Gao from Shiyanjia Lab (www.shiyanjia.com) for drawing schematic illustration. **Funding:** This work was supported by the National Natural Science Foundation of China grant 51776126. **Author contributions:** Supervision and funding: Z.H. Conceptualization: Z. Liu, Z.W., and Z.H. Preparation of colored fabrics: Y.L., S.Z., and Z. Liu Preparation of LIPSS metal sheets: R.L. and D.Z. MEMS TEG fabrication: E.M. and Z. Liu Characterization: Z. Liu, Y.L., S.L., and K.X. Writing: Z. Liu and Z.W. Review and editing: Z.H., D.Z., and Z. Li. **Competing interests:** The authors declare that they have no competing interests. **Data and materials availability:** All data needed to evaluate the conclusions in the paper are present in the paper and/or the Supplementary Materials.

Submitted 23 February 2022

Accepted 5 July 2022

Published 17 August 2022

10.1126/sciadv.abo7500